

M. FRAŠTIA

POSSIBILITIES OF USING INEXPENSIVE DIGITAL CAMERAS IN APPLICATIONS OF CLOSE-RANGE PHOTOGRAMMETRY

Marek Fraštia

Department of Surveying
Research field: Digital photogrammetry

Faculty of Civil Engineering
Slovak University of Technology
Radlinskeho 11, 813 68 Bratislava, Slovak Republic

ABSTRACT

The market offers many digital cameras a prices in a range from around 100 € up to and over 10 000 € (e.g., Hasselblad HD ~ 18 900 €). All these cameras can be used for the creation of models of special objects. Of course, differences in quality (= different prices) present different results. It is the purpose of this paper to outline the possibilities of inexpensive mid-range cameras (about 1 000 €) in applications of close-range photogrammetry, e.g., the creation of virtual spatial models of constructions, historical buildings and facades, models of small objects (< 1 m), industrial equipment, DEM of quarries and rock cuts, reconstruction of traffic accidents and crime sites, modeling of the human body, etc.

KEY WORDS

- digital photogrammetry
- digital camera
- calibration
- convergent photogrammetry
- test field

1. INTRODUCTION

The use of inexpensive cameras in close-range photogrammetry creates a problem of camera calibration in order to achieve good results. Other factors affecting the resulting accuracy include: the method of transformation into the referencing coordinate system, the amount and distribution of identical points, the resolution of digital images and the stability of the camera. The purpose of this paper is to determine the effect of factors involved in the process of creating a spatial model, beginning with photogrammetry up to the transformation into the reference coordinate system and to offer an optimal procedure to resolve the spatial position using the convergent photogrammetry method. For this purpose the calibration and test field (CTF) was used to help increase accuracy if inexpensive cameras are used.

2. CAMERA CALIBRATION

In order to calibrate non-metric cameras used for close-range

photogrammetry purposes, the procedures are not as standardized as those for metric aerial cameras. Depending on the accuracy required, the effectiveness and availability of the calibration equipment, various sophisticated attitudes towards the problem have been developed to solve issues involving the estimation of interior orientation elements and additional parameters.

Four concepts of camera calibration are used (Kraus, 1997):

- Calibration by a known spatial bundle of rays – comparison of the object and the image's angle with an optical axis.
- Calibration of the test field with known 3D coordinates – determination of the interior orientation parameters using Cartesian or polar coordinates.
- Calibration on the test field by means of known geometric relations in the object's area – introduction of constraints (e.g., right angle, planarity, co-linearity, etc.).
- Calibration on the test field with unknown coordinates – using the estimation of a free network.

The characteristics of these above mentioned concepts exploit the three basic calibration methods used in practice:



- laboratory calibration,
- on-the-job calibration,
- self-calibration.

As an alternative method, calibration by direct linear transformation (DLT) should be mentioned, which, however, gives results of a lower degree of accuracy compared with other methods and is preferably used for determination of the 3D position of points, when the interior orientation parameters are simultaneously resolved with unknown point coordinates.

The mathematical models are based on equations of the perspective transformation with additional parameters. The relation between the object coordinates (reference) and the corresponding image coordinates is expressed by the formula:

$$\begin{aligned} x' + \Delta x' &= x_0' - f \frac{m_{11}(X - X_0) + m_{21}(Y - Y_0) + m_{31}(Z - Z_0)}{m_{13}(X - X_0) + m_{23}(Y - Y_0) + m_{33}(Z - Z_0)} \\ y' + \Delta y' &= y_0' - f \frac{m_{12}(X - X_0) + m_{22}(Y - Y_0) + m_{32}(Z - Z_0)}{m_{13}(X - X_0) + m_{23}(Y - Y_0) + m_{33}(Z - Z_0)} \end{aligned} \quad (2-1)$$

Where x', y' are image coordinates, X, Y, Z are reference coordinates; x_0', y_0' are coordinates of the image principle point; f is the principal distance; $m_{11} - m_{33}$ are coefficients of the orthogonal rotation matrix; X_0, Y_0, Z_0 are reference coordinates of the projection centre, and $\Delta x', \Delta y'$ are corrections of the image coordinates involving different systematic errors.

There are many mathematical models approximating the distortion of an objective lens, the deflection of coordinate system axes or the affinity of an image. The user chooses and processes individual models depending upon the characteristics the camera uses. Distortion of the image is caused mainly by radial distortion, and the model mostly used for elimination of radial and decentering distortion is in the form of a polynomial:



Fig. 3-1 The calibration and test field - CTF

$$\begin{aligned} \Delta x' &= (x' - x_0') (K_1 r^2 + K_2 r^4 + K_3 r^6) + P_1 (r^2 + 2(x' - x_0')^2) + 2P_2 (x' - x_0')(y' - y_0') \\ \Delta y' &= (y' - y_0') (K_1 r^2 + K_2 r^4 + K_3 r^6) + P_2 (r^2 + 2(y' - y_0')^2) + 2P_1 (x' - x_0')(y' - y_0') \end{aligned} \quad (2-2)$$

Where K_i are coefficients of the radial distortion, P_i are coefficients of the decentering distortion and, r is the radial distance.

It is the purpose of this paper to test different effects on the resulting reference spatial accuracy by means of:

- calibration with known reference coordinates,
- self calibration – all images have equal parameters of interior orientation,
- self calibration – every image has its own parameters of interior orientation,
- the DLT method

3. TESTING OF DIGITAL CAMERAS

Finding out the appropriateness of a digital camera for close-range applications requires testing the camera itself as well as the corresponding methods of calibration and processing attitudes with regard to the resulting accuracy. It is quite interesting to compare the actual accuracy with the accuracy of any software used, which enables evaluation the reliability of the results. Calibration and test fields are used for this purpose.

3.1 Calibration and test field

The calibration and test field (figure 3-1) designed by the author at the Faculty of Civil Engineering STU in Bratislava for the calibrating cameras as well as for the evaluation of the accuracy of

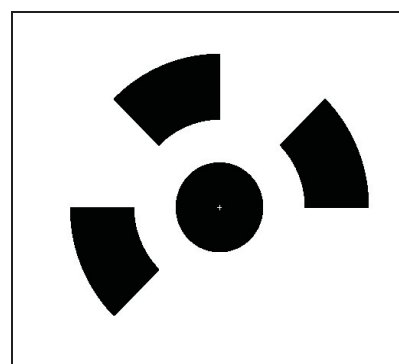


Fig. 3-2 12-bit coded target

photogrammetric measurements has the following characteristics:

- a guarantee of high dimensional stability (2 sub-basement of the Faculty of Civil Engineering A block),
- a good spatial arrangement,
- 114 test points marked by coded circular targets on plastic material,
- 3x4x2.5 m³ dimensions of the test field,
- minimal intersection angle 45⁰, maximal intersection angle 60⁰,
- maximal object distance 5 m,
- the test field is imaged on the frame of a wide angle camera,
- known referenced coordinates of all points, determined with an accuracy of $m_x, m_y, m_z < 0.1$ mm.

The coded targets (EOS Systems Inc., 2005) seen in figure 3-2 enables the automatic identification and measurement of points and thereby greatly accelerates the calibration process or the spatial determination of points and yields about a 3 to 10 times higher accuracy.

3.2 Taking pictures

For every test a total of 7 exposures from different stations were taken, with one of them being rotated $\kappa = 90^0$ (figure 3-3). Methodically it is convergent photography with a general orientation of the camera axis. The camera was fixed on a tripod, and the camera settings for every exposure were (within the limits of the camera used):

- maximal f-stop due to the depth of the field,
- minimal ISO to reduce any noise,
- fixed focus.

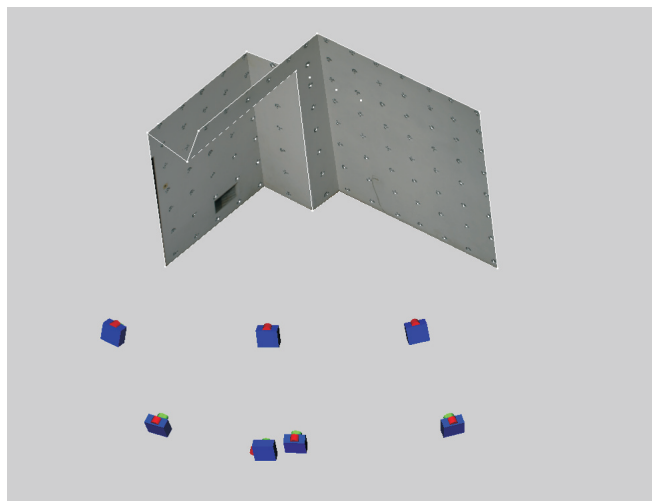


Fig. 3-3 Configuration of the camera stations

3.3 Photogrammetric processing

The image processing was performed using "PhotoModeler Pro5" (PM5) software for digital photogrammetry.

An overview of the digital image processing within the PM5 environment includes the following steps:

- project name and reading the image data,
- automatic identification and measurement of the points observed with a sub-pixel accuracy (of 0.1 pixel),
- manual sub-pixel measurement of points not found or not correctly identified by the software (in 15%),
- import of reference coordinates of the points observed and marking the control points on the image as fixed points, i.e., without changing their position after adjustment (hard positioning),
- calculations – common adjustment of a bundle of rays with simultaneous camera calibration – the operator selects parameters of the inner orientation as determined by the calibration,
- checking the results.

Geodetic and photogrammetric measurements produce two basic data sets – spatial coordinates determined by both methods. Assuming the accuracy of the Cartesian geodetic coordinates is $m_{xg} = m_{yg} = m_{zg} \leq 0.1$ mm and the expected accuracy of the coordinates as determined by the photogrammetry is no better than $m_{xf} = m_{yf} = m_{zf} \sim 0.6$ mm, then the differences in the coordinates:

$$X_g - X_f = \epsilon_x, \quad Y_g - Y_f = \epsilon_y, \quad Z_g - Z_f = \epsilon_z \quad (3-1)$$

can be considered as true errors of the photogrammetric method. The random character of these errors allows to be dealt with the normal (Gauss) distribution of random quantity and their mean value $E(\epsilon_x) = E(\epsilon_y) = E(\epsilon_z) = 0$. Then the real accuracy of the photogrammetric method used under the given conditions is expressed by the empirical mean error $\sigma_x, \sigma_y, \sigma_z$ resulting from the differences $\epsilon_x, \epsilon_y, \epsilon_z$ for the individual coordinate axis. The important characteristics are as well as the maximal differences $\epsilon_{xmax}, \epsilon_{ymax}, \epsilon_{zmax}$ with values no greater than the accuracy of the corresponding coordinates.

The characteristics of the differences between the geodetic and photogrammetric coordinates are:

- The mean value is the arithmetic mean of all the coordinate deviations for each coordinate axis

$$E(\epsilon_x) = \frac{\sum \epsilon_x}{n}, \quad E(\epsilon_y) = \frac{\sum \epsilon_y}{n}, \quad E(\epsilon_z) = \frac{\sum \epsilon_z}{n} \quad (3-2)$$

The greater incidental deviation from the zero value signalizes the possible systematic character of the population of the deviations.



- The empirical mean error expresses the total actual accuracy of the photogrammetric coordinates

$$\sigma_x = \sqrt{\frac{\sum(\epsilon_x)^2}{n}}, \sigma_y = \sqrt{\frac{\sum(\epsilon_y)^2}{n}}, \sigma_z = \sqrt{\frac{\sum(\epsilon_z)^2}{n}} \quad (3-2)$$

- The maximal deviation expresses the most divergent values of the plus and minus deviations from the reference coordinates
- The maximal mean error of the transformation expresses the accuracy of the transformed points (not residual at identical points). This accuracy is calculated by the software and does not exceed 1.2 times the mean error of all the points.
- The maximal mean error of PM5 expresses the maximal value of the mean error calculated by the software and does not exceed 1.2 times the mean error of all the points. This value as compared with the actual accuracy indicates confidence in the characteristics estimated by the software.

3.4 Effect of the calibration method on the results

The results of the calibration methods: calibration from the reference coordinates (CRC); self-calibration – all the photos have the same interior orientation (SC); self-calibration separately – every photo has its own interior orientation (SCS); and calibration by direct linear transformation (DLT) on 8 control points optimally distributed are compared in Figure 3-4.

The characteristics of the results:

- the most accurate calibrations were by SCS and CRC with a good coincidence of the theoretical and actual accuracy as well,
- the results of the SC calibration were approximately 1.5 times

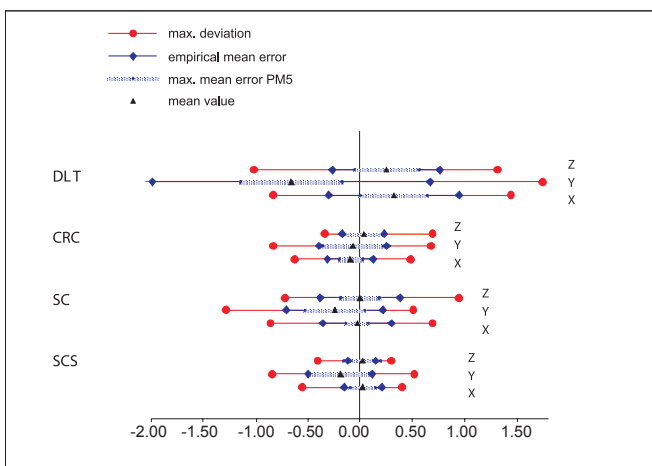


Fig. 3-4 Comparing the methods of calibration

worse, but can be considered as very good in spite of the slightly overestimated a priori accuracy,

- The CRC, SC and SCS methods indicated a good homogeneity in all the axes of the reference coordinate system; the mean values of the deviation involve no significant systematic translation (>3*reference),
- the DLT method is not suitable for applications with the highest required accuracy,
- SC and SCS methods are, from the point of view of the effectiveness, the most suitable, especially, for objects with a substantially different dimension compared with the calibration and test field and with a sufficient number of points,
- objects with similar dimensions such as those of CTF and with fewer points (< 30 points) are recommended to be processed with interior orientation parameters determined using CTF,
- for unstable cameras with a variable focus or for processing objects using different cameras, the SCS calibration is the most suitable.

3.5 Effect of transformation on results

The empirical mean error was computed from differences in the coordinates. Two transformation methods were compared – perspective transformation (PT) as a direct transformation to the reference system and the spatial similarity transformation (ST) after the PT on a free network. Six control points and CRC were used as a calibration method.

A comparison of the test results of the transformation methods into the reference coordinate system confirmed that the free network method in this case did not produce the most accurate results; to the contrary it is as much as 5 times (worse) less accurate than that of the perspective transformation directly into the reference coordinate system. It is evident that the resulting spatial position of the points

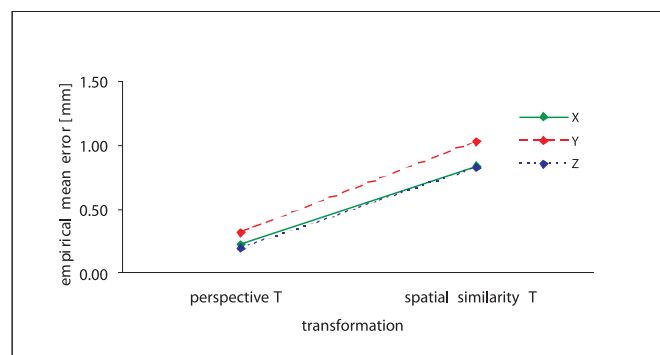


Fig. 3-5 Effect of the transformation method on empirical mean error

was affected by some unknown systematic errors which caused the model's deformation.

3.6 Effect of the number of control points on the results

The effect of the number of control points of both transformations was analyzed. In figure 3-6 the empirical mean error can be seen according to the number of the CPs using the perspective transformation and after the SCS calibration. In figure 3-7 empirical mean error can be seen according to the number of the CPs using the spatial similarity transformation and after the CRC calibration.

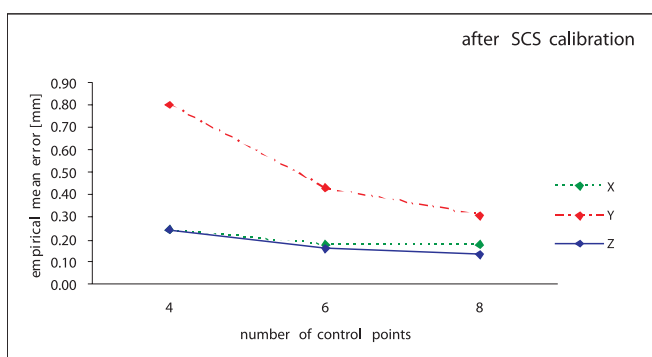


Fig. 3-6 Effect of the number of control points from the perspective transformation

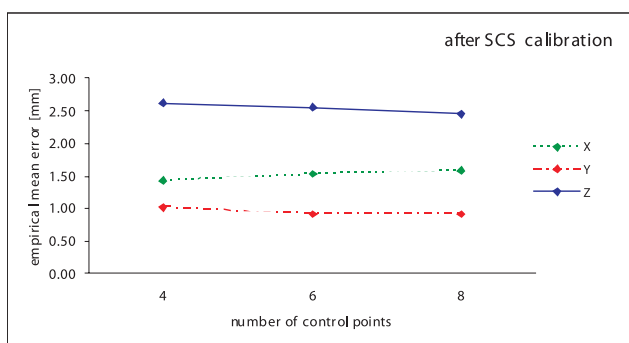


Fig. 3-7 Effect of the number of control points from the spatial similarity transformation

The characteristics of the results:

- a different number of identical points of the spatial transformation (4, 6, 8 points) has no significant effect on the resulting accuracy of the reference coordinates. Increasing the number of identical points is not effective,

- increasing the accuracy of the perspective transformation is evident from the use 6 control points. The higher number of control points has only a negligible effect on the resulting accuracy of the reference coordinates. Therefore, the recommended number of control points is 6 with regard to the accuracy, over the determination and elimination of casual gross errors. Increasing the number of control points is not effective.

3.7 Effect of image compression and resolution on the results

It is interesting to find out the effect of the image compression on the resulting accuracy according to the size of raster files. The compression in the JPEG format (super high quality -SHQ, high quality - HQ) compared with the TIFF uncompressed format as well as the effect of the change of the image resolution by interpolation (standard quality - SQ1).

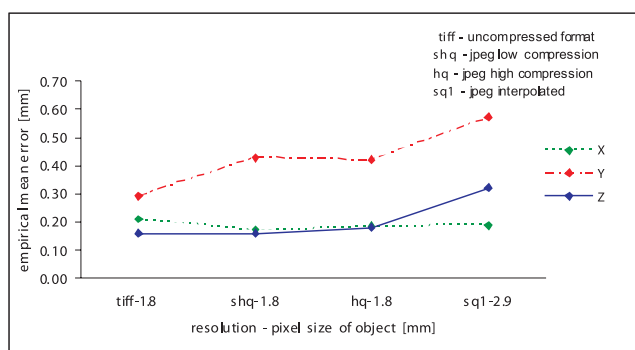


Fig. 3-8 Effect of compression and resolution on empirical mean errors

The characteristics of the results:

- according to expectations, the best results were obtained with the TIFF format, first of all, by the mean empirical error,
- compression of the image (at the same resolution does not have a significant effect on the resulting accuracy),
- the change in the resolution (TIFF vs. SQ1) in the Y and Z axes is expressed according to the assumption in relation 1:1.6, which is the ratio of the pixel size to the object 1.8:1.9. Along axis X the accuracy's the same,
- the lower quality in the Y axis is given by the intersection angle.

3.8 Comparison of different cameras

Accessible digital cameras mid and low-range class were tested and classified as inexpensive cameras. The characteristics of the



Table 3-1 Characteristics of data formats tested

OLYMPUS C-8080 Wide Zoom					
Data format	name	compression	number of pixels	pixel	file size [MB]
[μm]					
TIFF	TIFF	without compression	3264 x 2448	2.7	24
JPG	SHQ	low compression	3264 x 2448	2.7	3
JPG	HQ	high compression	3264 x 2448	2.7	1.3
JPG	SQ1	interpolation	2048 x 1536	4.3	0.5

Table 3-2 Characteristics of the cameras tested

Camera	Format	f [mm]	sensor [mm]	pixel on CTF [mm]
Olympus C-8080	professional compact, 8 MP	7.4	8.8 x 6.6	1.8
Canon EOS D300	SLR mirror, 6 MP	18.7	22.6 x 15.1	2.0
Sony DSC P-150	amateur compact, 7 MP	7.9	7.0 x 5.3	1.4
Olympus C-990	amateur compact, 2.1 MP	6.0	5.6 x 4.2	2.9

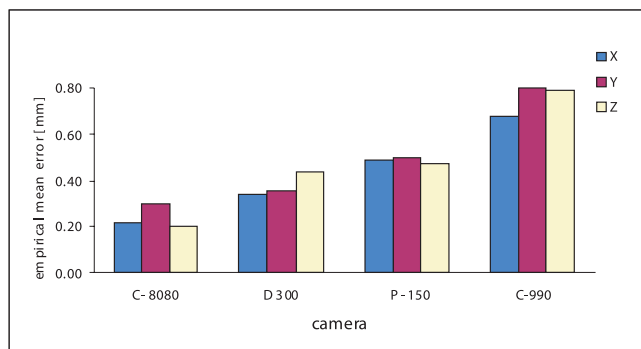


Fig. 3-9 Comparison of different cameras

cameras are in table 3-2. All the cameras were calibrated by the SCS method; pictures had a maximal resolution in the JPG format. The perspective transformation on 6 control points was used as a reference transformation method.

The characteristics of the results:

- as expected, the worst results were given by the 2.1 Mpix compact C-990 camera, which, with regard to its size, is usable only for a lower degree of accuracy,
- a comparison of the compact vs. mirror camera types yields a better ranking for the Olympus C-8080 compact camera with an object pixel size of about equal value,

Table 3-3 Relative accuracy of the cameras

Camera	C-8080	D 300	P-150	C-990
Relative accuracy	1:16 000	1:12 000	1:10 000	1:8 000

- the Sony P-150 camera having the best resolution in the object space, placed in the ranking after C-8080 and D-300 cameras. The explanation can be in the low stability of the interior orientation parameters caused by refocusing among the individual exposures.

The relative accuracy (table 3-3) expresses the accuracy achievable with regard to the object's distance (e.g., 1:10 000 represents the accuracy of 1 mm at a 10 m distance).

3.9 Project to determinate a highly accurate model by digital close-range photogrammetry

Based on the experience and results mentioned above, we can propose procedures for determining the spatial position of the point (object) with the highest attainable accuracy under the conditions given. The object – CTF and the Olympus C-8080 digital camera are available. Then, within the complete process of determining spatial position as the most suitable procedure, the following can be considered:

1. Convergent photography as a photogrammetric method.

2. Images saved in the TIFF format (assuming that there is a sufficient memory capacity and an efficient PC and software) or JPEG with low compression.
3. When possible, 6 control points are to be distributed, framing the whole object and marked by code targets which have been determined in the reference coordinate system with a 2 times greater accuracy than the required accuracy of any unknown points.
4. Pre-calibration of the compact camera by self-calibration (SC).
5. Calculation of the photogrammetric coordinates directly by the perspective transformation on the control points using on-the-job self-calibration.

Using this procedure the best results (the highest accuracy) were obtained.

Table 3-4 Statistical evaluation of the results

$\sigma_0 = 0.021$	X	Y	Z
Max. deviation „+“ [mm]	0.32	0.78	0.43
Max. deviation „-“ [mm]	-0.49	-0.70	-0.51
Mean value [mm]	-0.14	-0.17	-0.06
Empirical mean error [mm]	0.16	0.24	0.15
σ PM5 [mm]	0.15	0.34	0.24
Average deviation [mm]	0.13	0.19	0.12
Max. correction [pix]	0.47		
Standard deviation [pix]	0.09		

Figure 3-10 shows a histogram of the frequency of all the differences e_x, e_y, e_z at an interval of 0.05 mm. All the differences represent the mean value $E = -0.12$ mm and the empirical mean error $\sigma = 0.32$ mm.

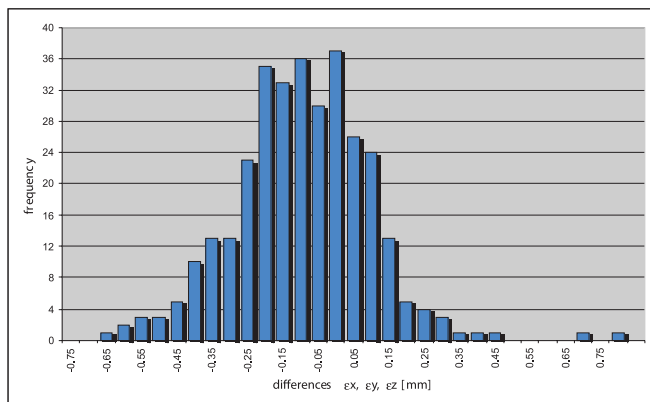


Fig. 3-10 Frequency histogram of coordinate differences

The following frequencies of the 324 differences in percentage are in Table 3-5:

Table 3-5 Percentage of frequency of differences

$\sigma_e = 0.32$ [mm]	$1*\sigma$	$2.5*\sigma$	$3*\sigma$
Frequency [%]	85.5	99.1	100

In general, the photogrammetric results obtained can be considered as very accurate with regard to the camera used. The ratio of the time requirements between the photogrammetric and geodetic methods for the determination of all the points was 1:4 (including the geodetic measurement of the control points). Naturally, by increasing the image scale, the geodetic methods could not achieve the accuracy of photogrammetric measurements.

4. APPLICATIONS

In order support the results mentioned in the paper, three examples exploiting the Olympus C-8080 digital camera and the Photomodeler software are presented.

4.1 The wall of the "Kasárne" structure in the Trenčín castle

The wall of a former garrison in the structure of the Trenčín castle was photogrammetrically documented for reconstruction as part of a project for tourist accommodation. The length of the wall is 50m, the height is 11 m and its thickness varies between 0.5 and 1.2 m. The ground plane has the shape of the letter "S". The spatial shape of the wall was determined using geodetic documentation and planimetry in the local coordinate system and the orthophotomap as an orthogonal projection into a vertical plane parallel with the line connecting the boundaries of the wall (Figure 4-1). Convergent photography with a general orientation of the camera axis was used. All the structure's points have been defined as natural targets, and the spatial accuracy of the model is up to 2 cm. The textured, virtual 3D model of the wall is presented in figure 4-2.

4.2 Testing solids for laser scanners

For analyses of terrestrial laser scanner results, it was necessary to reconstruct the accurate spatial shape of testing solids. The dimensions of the solids are:

- prisms: 450 x 450 x 500 mm³, 2500 points,
- cylinders: diameter = 250 mm, height = 500 mm, 1800 points.



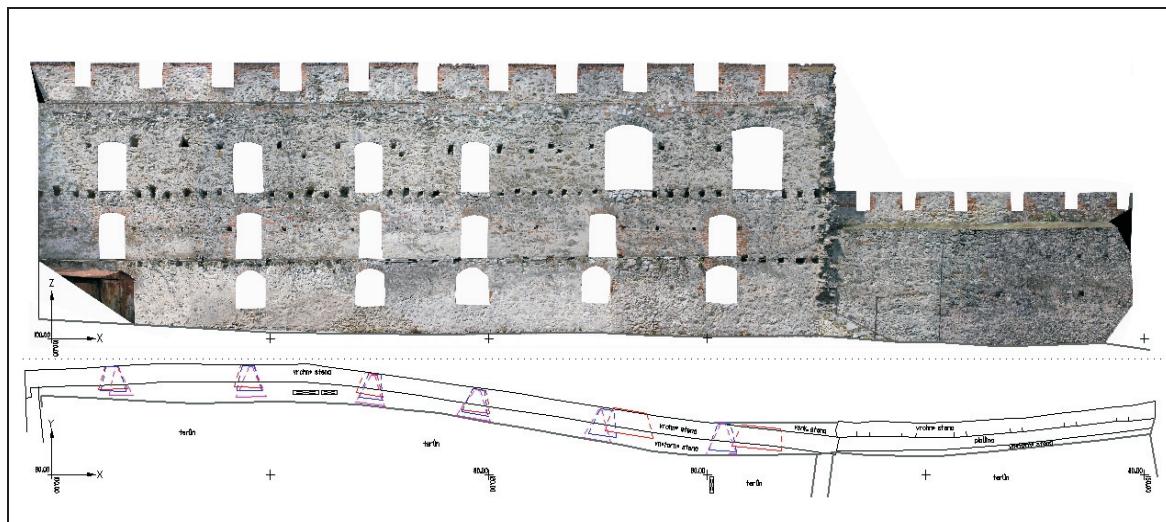


Fig. 4-1 Orthophotomap of wall of the Kasárne in the Trenčín castle

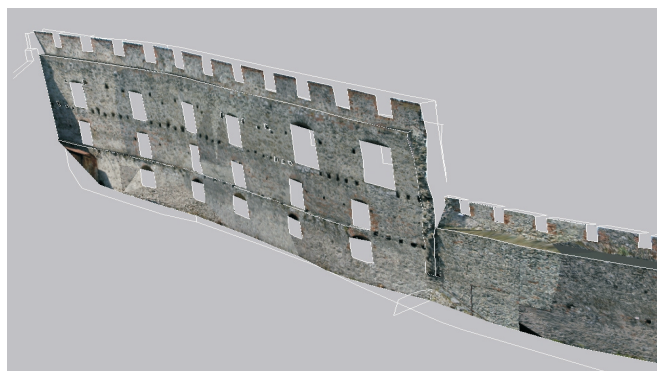


Fig. 4-2 Textured virtual 3D model

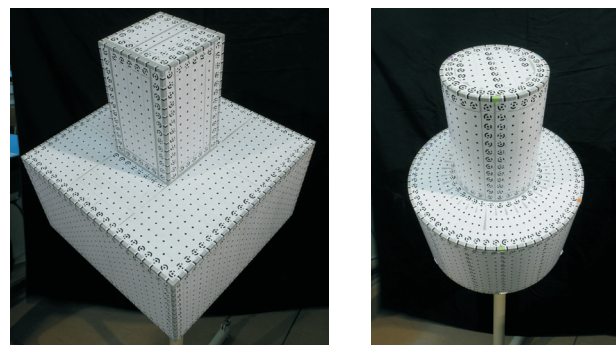


Fig. 4-3 Original images

On the surfaces of the solids were black circular targets and along the edges were rectangular black and white targets. Figure 4-3 presents the original images of the solids. The model in the form of a vector can be seen in figure 4-4, and the textured virtual model is shown in figure 4-5. The spatial accuracy obtained on the surfaces due to the automatic measurement of the circular targets varies up to 0.06 mm and, on those surfaces along the edges (manual measurement), up to 0.3 mm.

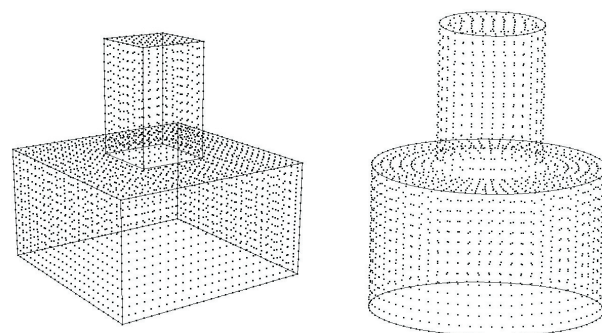


Fig. 4-4 Vector models

4.3 The APOLLO bridge in Bratislava

The new APOLLO bridge in Bratislava has been experimentally reconstructed using convergent photogrammetry (Fraštia, 2005).

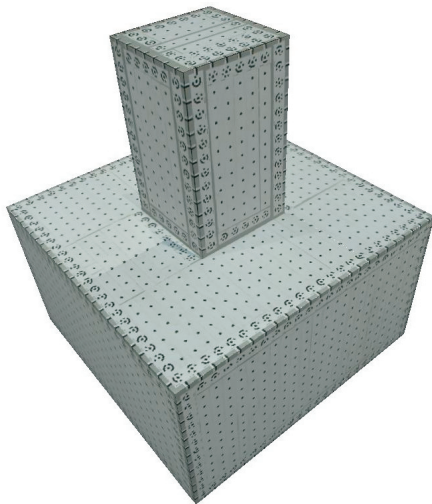


Fig. 4-5 Textured virtual 3D model

The length of the reconstructed segment is around 230 m, and 12 images were used. A spatial point precision of up to 5 cm was achieved. The virtual model is shown in figure 4-6.

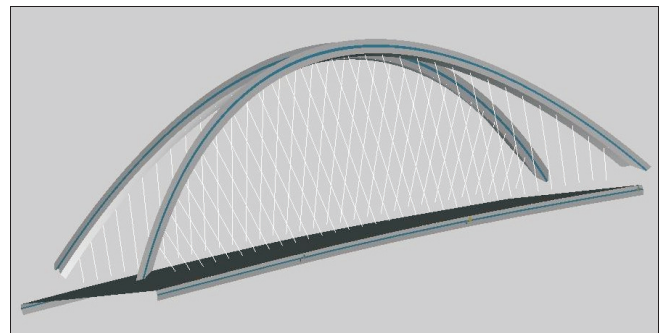


Fig. 4-6 Partial 3D virtual model of the APOLLO bridge

5. CONCLUSION

In all probability we can assume that the results presented in the paper show the remarkable possibilities of using inexpensive digital cameras used for in close-range photogrammetry applications. The evidence presented in the figures and tables seems to suggest that involvement of the CTF in digital data processing guarantees a high accuracy of the results.

REFERENCES

- **EOS Systems Inc. (2005)** PhotoModeler Pro5: User Manual.
- **Fraštia, M. (2005)** Production of the model of the Apollo bridge's structure using digital photogrammetry. In: Geodézia a kartografia v doprave, pp. 39-44 (in Slovak).
- **Kraus, K. (1997)** Photogrammetry: Advanced Methods and Applications. 1st english ed. Bonn: Dümmler, 1997, 466 pp.

